ChemComm

COMMUNICATION

View Article Online
View Journal | View Issue

Cite this: *Chem. Commun.*, 2015, **51**, 15012

Received 15th June 2015,
Accepted 17th August 2015

DOI: 10.1039/c5cc04936a

www.rsc.org/chemcomm

A sea anemone-like CuO/Co_3O_4 composite: an effective catalyst for electrochemical water splitting†

Xiumin Li,[a] Guoqing Guan,*[ab] Xiao Du,[bc] Ji Cao,[a] Xiaogang Hao,[c] Xuli Ma,[bc] Ajay D. Jagadale[b] and Abuliti Abudula[ab]

A facile unipolar pulse electrodeposition combined with the thermal oxidation method was applied for fabrication of CuO/Co_3O_4 composites on carbon electrode for water electrolysis, and it was found that the sea anemone-like one with a 3D hierarchical structure formed at −0.8 V exhibited excellent performance for water electrolysis at a low overpotential with high stability.

Hydrogen is an ideal candidate for the replacement of fossil fuel energy in the future due to zero emission of the carbonaceous species during its utilization. Hydrogen production *via* electrochemical splitting of water using natural energy resources such as solar and wind energy has attracted increasing interest. In the course of seeking highly efficient catalysts for water electrolysis, the biggest challenge is to reduce the amount of noble metals[1] used in the electrode or to replace them with inexpensive materials.[2] However, non-precious materials always have lower activity than noble metals. To resolve this problem, increasing the number of active sites of these materials by fabrication of three-dimensional (3D) nanostructures has been found to be an efficient approach.[3] In particular, the direct fabrication of these materials with 3D branched core/shell heterostructures on a conductive substrate is of great interest because it could result in a larger surface area for efficient transport of electrons, ions and generated gases in the electrode which is beneficial for maximizing the utilization of these water electrolysis materials.[3,4] Moreover, nanostructured hybrid materials with two or more components could show synergetic properties through the reinforcement or modification of each other.[5] To date, various electrodes with 3D heterostructures have been developed and have shown amazing enhanced properties for water electrolysis. For instance, Chen *et al.*[3] and Liu *et al.*[6] respectively synthesized $NiCo_2O_4$ and α-Fe_2O_3 nanorod arrays on carbon cloth as the anode for the oxygen evolution reaction (OER), and found that a current density of 10 mA cm^{-2} in an alkaline electrolyte can be achieved at overpotentials of 320 and 420 mV, respectively. Shi *et al.*[7] prepared tungsten nitride nanorods array on carbon cloth as the cathode for hydrogen evolution with high catalytic activity at all pH values. Cheng *et al.*[4] *in situ* grew a core/shell nanorod array consisting of $Cu(OH)_2$–CuO nanosheets as the shell and Cu as the core on Cu foil, and found that a current density of 10 mA cm^{-2} could be obtained at an overpotential of 417 mV with a long-term stability (at least 22 h) of catalytic activity. Nevertheless, numerous efforts are still required for the facile and controllable synthesis of hybrid heterostructures with a well-defined morphology at low growth temperature for large scale water electrolysis.

Recently, the earth-abundant Fe, Co, Ni and Mn oxides have been investigated as potential electrocatalysts for water splitting.[6,8–10] Among them, cobalt oxides are found to be promising bifunctional catalysts for water electrolysis under the same conditions.[2,9] The abundant and diversiform d-orbitals endow cobalt oxides with the highly active sites for electrocatalytic water splitting.[11,12] Fabrication of CuO/Co_3O_4 nanowire heterostructures using the thermal oxidation method has been recently reported,[5] which show a high performance in lithium ion battery applications; such a class of materials could be also applied for water electrolysis. In this study, a facile unipolar pulse electro-deposition (UPED) combined with thermal oxidation method has been applied for the fabrication of a CuO/Co_3O_4 composite on a carbon electrode. It is expected that a hierarchical CuO pillar@Co_3O_4 nanosheet core/shell array on the electrode with high catalytic activity for water electrolysis can be obtained.

The $Cu/Co(OH)_2$ precursor of the CuO/Co_3O_4 composite is prepared by UPED on a carbon rod (CR) electrode, and the procedure follows the method described in detail elsewhere.[13] Herein, the potentials applied during the on-time operation ranged from −0.2 to −1.2 V. Other parameters, *i.e.*, pulse duration, pulse cycle times

[a] *Graduate School of Science and Technology, Hirosaki University, 1-Bunkyocho, Hirosaki 036-8560, Japan*
[b] *North Japan Research Institute for Sustainable Energy (NJRISE), Hirosaki University, Matsubara, Aomori 030-0813, Japan. E-mail: guan@hirosaki-u.ac.jp; Fax: +81-17-735-5411*
[c] *Department of Chemical Engineering, Taiyuan University of Technology, Taiyuan 030024, China*

† Electronic supplementary information (ESI) available: Experimental section and optimization of preparation parameters, BET, EDS, EIS, durability and O_2 productivity of CuO/Co_3O_4 composites. See DOI: 10.1039/c5cc04936a

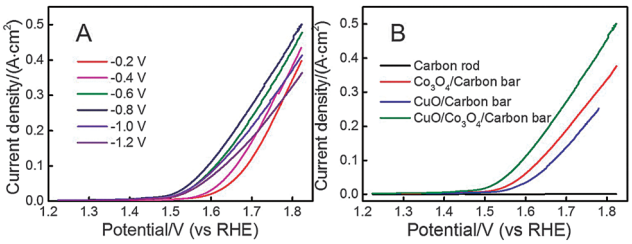

Fig. 1 (A) Polarization curves of CuO/Co_3O_4 composite catalysts prepared at different potentials; (B) polarization curves of the carbon rod substrate, and Co_3O_4, CuO and CuO/Co_3O_4 composite catalysts prepared at −0.8 V in 1 M KOH solution, scan rate: 2 mV s^{-1}.

and concentration of preparation solution are optimized. It is found that the electrode with the highest catalytic performance is obtained when the pulse duration, pulse cycle times are 1 s and 500 in the solution of 0.1 M $Co(NO_3)_2$ and 0.05 M $Cu(NO_3)_2$ (for details of experiment and optimization, see ESI†).

As shown in Fig. 1, the electrolysis performance tests of CuO/Co_3O_4 composites, pure CuO and Co_3O_4 electrodes are carried out using the linear sweep voltammetry (LSV). Obviously, the catalytic activity of the composite electrode is highly dependent on the deposition potential. The CuO/Co_3O_4 composite prepared at −0.8 V shows the best catalytic performance for OER with a lower overpotential to afford the same current density. For comparison, catalytic properties of pure CuO and Co_3O_4 were tested. As shown in Fig. 1B, CuO and Co_3O_4 both show electrochemically active toward the OER, the overpotentials of 312 mV and 284 mV, respectively, are needed to afford a current density of 10 mA cm^{-2}. In contrast, the CuO/Co_3O_4 composite electrode exhibits greatly enhanced catalytic activity with an overpotential of only 227 mV to drive the same current density. This overpotential is much lower than those of the previously reported OER catalysts under alkaline conditions, including CCHH/MWCNT (285 mV),[14] $NiCo_2O_4$ (320 mV),[3] Co_3O_4 (320 mV),[9] Cu/($Cu(OH)_2$–CuO) (417 mV),[4] Mn_3O_4/$CoSe_2$ (450 mV),[10] α-Fe_2O_3 NA/CC (420 mV),[6] α-MnO_2–SF (490 mV),[15] and is comparable to the best values reported, such as those of NiFe–LDHs (235 mV),[16] NiFe–GO–LDHs (206 mV)[17] and NiFe–CNT–LDHs (223 mV).[8] O_2 productivity of CuO/Co_3O_4 composite electrodes is also measured (Fig. S4, ESI†), and the composite exhibits a high Faraday efficiency of 95%.

This excellent catalytic performance may be attributed to the microstructure and morphology of the Co_3O_4 and CuO materials. Fig. 2 shows SEM images of pure CuO, Co_3O_4 and CuO/Co_3O_4 composite prepared by UPED under different applied potentials. The pure CuO material (Fig. 2A) shows a large-size particle structure which might be accumulated by irregular lumps, due to the fast reaction rate of Cu^{2+} reduction while the pure Co_3O_4 material (Fig. 2B) obtained under the same conditions shows a uniform meshy nanosheet structure which could provide more active sites for water electrolysis. Interestingly, the morphology and structures of CuO/Co_3O_4 composite materials are completely dependent on the pulse potential. At the applied potential of −0.2 V (Fig. 2C), smooth CuO nanorods with a diameter of about 200 nm and some pandan leaf-like arrays several micrometers in length are formed on the electrode, where the arrays grow in a dispersed

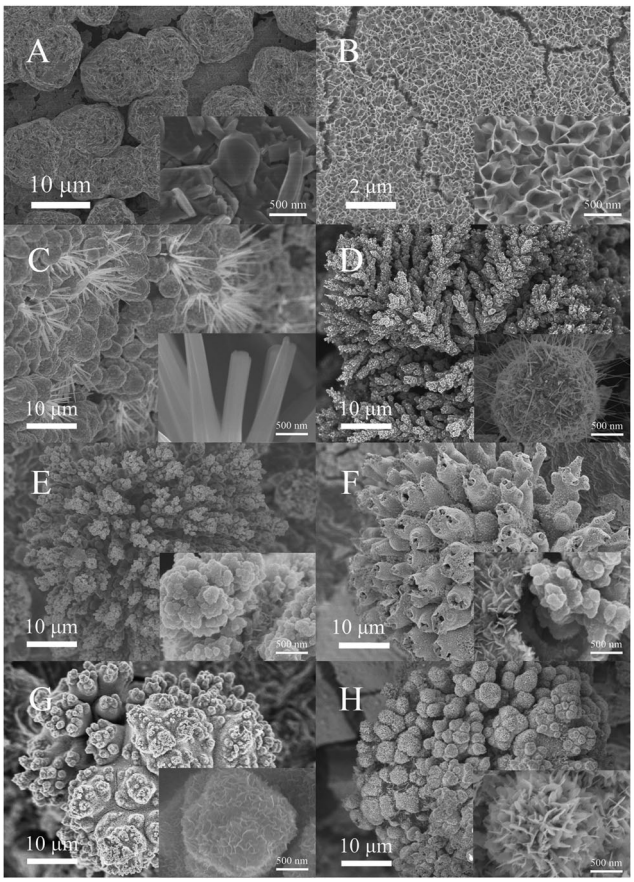

Fig. 2 SEM images of pure CuO (A), Co_3O_4 (B) and CuO/Co_3O_4 composite catalysts (C–H) obtained at different preparation potentials (C: −0.2 V, D: −0.4 V, E: −0.6 V, F: −0.8 V, G: −1.0 V, H: −1.2 V). Insets show enlarged images.

and random manner. At the applied potential of −0.4 V (Fig. 2D), a pine needle-like morphology is obtained, in which the sphere is covered by slender thorns. At the applied potential of −0.6 V (Fig. 2E), a dispersive branch structure with a stamen-like array appears, in which the composite is composed of nanoparticles and nanosheets, and the particle size is much smaller than the one obtained at −0.4 V. Similar particles with a looser combination with a 3D structure are formed on the electrode at −0.8 V. As shown in Fig. 2F, 3A and B, a sea anemone-like core–shell structure formed by nanosheets growing around the inside of the particles uniformly is obtained, which showed a hierarchical core/shell array consisting of nanosheets as the shell and nanoparticles as the core. Further changing the potentials to −1.0 V and −1.2 V, the dispersive branch structure disappears and a large-size accumulational morphology is obtained (Fig. 2G and H, Fig. S5, ESI†), which may be not be beneficial for electrons and electrolyte circulation.

Stimulated by this novel 3D hierarchical core/shell array architectures (Fig. 3A and B), the CuO/Co_3O_4 composite obtained at −0.8 V is characterized by BET, XRD, EDS, TEM and SEM with higher magnification. Revealed by BET results (Fig. S6, ESI†), the CuO/Co_3O_4 composite shows a higher surface area (168.5 m^2 g^{-1}) than pure CuO (114.4 m^2 g^{-1}) and Co_3O_4 (153.6 m^2 g^{-1}) materials, and the pore sizes of the composite range in 3–16 nm. Fig. 3(C) shows the high resolution TEM

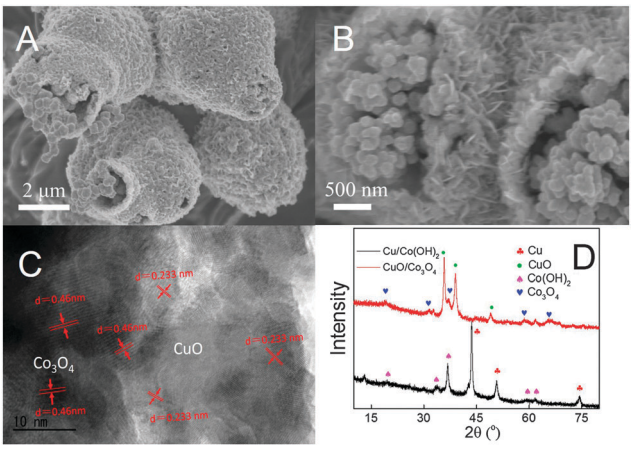

Fig. 3 Different magnification SEM images (A and B) and TEM image (C) of CuO/Co_3O_4 composite catalysts with a sea anemone-like morphology. (D) XRD patterns of CuO/Co_3O_4 composite catalyst before and after calcination.

image of the composite. The well-resolved lattice fringes with the interplanar spacing of 0.233 nm and 0.46 nm correspond to the (111) plane of CuO[4] and the (111) plane of Co_3O_4,[5] respectively, strongly supporting the formation of the CuO–Co_3O_4 composite phase. The XRD patterns of the composite before and after calcination are shown in Fig. 3D. One can see that the composite is composed of all peaks of Cu[4] and $Co(OH)_2$[18] crystals before the calcination, but change to CuO[4] and Co_3O_4[11] crystals after the calcination. As revealed by EDS spectra (Fig. S7, ESI†), which are obtained by detecting the pillar core and nanosheet shell respectively, the core pillar mainly consists of Cu and O elements while the nanosheet shell consists of Co, O and a trace amount of Cu elements. Combined with XRD data, one can confirm that the hierarchical core/shell array obtained at −0.8 V consists of Co_3O_4 nanosheets as the shell and CuO pillar as the core. This kind of a structure provides a series of advantages for water electrolysis. Firstly, both CuO and Co_3O_4 catalysts show good catalytic performance for OER. Compared with pure CuO and Co_3O_4 catalysts, the composite obtained exhibits a smaller size of CuO nanoparticles and Co_3O_4 nanosheets, which should be beneficial for exposing more active sites.[5] Secondly, the direct growth of $Cu/Co(OH)_2$ precursor on CR by one-step electrodeposition ensures good interface connection between them, facilitating electrons flowing from the catalyst array to the current collector during anodic polarization. Thirdly, the porous core/shell array configuration largely increases the amount of contact areas between electrolyte and active sites, and the large surface area greatly facilitates ion and electron diffusion. Meanwhile, the inside CuO pillars not only serve as a physical support for this class of nanoarrays but also provide the channels for electron transport, and simultaneously, the highly porous Co_3O_4 nanosheets are well wrapped around the CuO pillars, which favors the exposure of more active sites and thus enhances catalytic activity per geometric area. Fourthly, the open spaces between neighboring composite branches facilitate the diffusion of electrolyte and generation of oxygen. Finally, the binder-free nature avoids the increase of various transfer resistances and the blockage of active sites and the inhibition of diffusion.

Electrochemical impedance spectroscopy (EIS) of CuO/Co_3O_4 composite and those of pure CuO, Co_3O_4 electrodes are provided in Fig. S8, ESI.† As expected, the CuO/Co_3O_4 electrode exhibits the lowest charge transfer resistance (R_{ct}) of 0.29 Ω, while the R_{ct} of CuO and Co_3O_4 are 1.57 and 0.35 Ω respectively, implying that CuO/Co_3O_4 has lower charge transfer resistance through a mutual reinforcement and/or modification of CuO and Co_3O_4. The time-dependent current density curve of the CuO/Co_3O_4/CR electrode is collected at 1.8 V (Fig. S8, ESI†) where the cell shows a high hydrogen evolution rate. Only a slight fluctuation of the current is observed during 16 h, indicating that such a composite electrode is capable of maintaining its catalytic activity for a long time.

In summary, CuO/Co_3O_4 composite catalysts with various novel morphologies were synthesized using a facile unipolar pulse electrodeposition method combined with the thermal oxidation method. The morphology and microstructure of composite materials are highly dependent on the preparation potential. It is found that the sea anemone-like one with a 3D hierarchical structure is formed at −0.8 V. Benefiting from its smart hybridization of CuO pillar@Co_3O_4 nanosheet core/shell array, a remarkably enhanced catalytic performance for OER is obtained. In addition, this electrode reveals low charge transfer resistance and excellent long-term durability. In view of the facile and efficient fabrication process and the low-cost nature of Cu and Co oxides, this material has great potential to be an inexpensive catalyst toward electrochemical water splitting.

This work was supported by Sekihiyo Facility Industrial Co., Ltd.

Notes and references

1 D. V. Esposito, S. T. Hunt, Y. C. Kimmel and J. G. Chen, *J. Am. Chem. Soc.*, 2012, **134**, 3025–3033.
2 S. Cobo, J. Heidkamp, P.-A. Jacques, J. Fize, V. Fourmond and L. Guetaz, and B. Jousselme, *Nat. Mater.*, 2012, **11**, 802–807.
3 R. Chen, H. Y. Wang, J. Miao, H. Yang and B. Liu, *Nano Energy*, 2015, **11**, 333–340.
4 N. Cheng, Y. Xue, Q. Liu, J. Tian, L. Zhang, A. M. Asiri and X. Sun, *Electrochim. Acta*, 2015, **163**, 102–106.
5 J. Wang, Q. Zhang, X. Li, D. Xu, Z. Wang, H. Guo and K. Zhang, *Nano Energy*, 2014, **6**, 19–26.
6 Q. Liu, A. M. Asiri and X. Sun, *Electrochem. Commun.*, 2014, **49**, 21–24.
7 J. Shi, Z. Pu, Q. Liu, A. M. Asiri, J. Hu and X. Sun, *Electrochim. Acta*, 2015, **154**, 345–351.
8 M. Gong, Y. Li, H. Wang, Y. Liang, J. Z. Wu, J. Zhou, J. Wang and T. Regier, *J. Am. Chem. Soc.*, 2013, **135**, 8452–8455.
9 S. Du, Z. Ren, J. Zhang, J. Wu, W. Xi, J. Zhu and H. Fu, *Chem. Commun.*, 2015, **51**, 8066–8069.
10 M. R. Gao, Y.-F. Xu, J. Jiang, Y. R. Zheng and S.-H. Yu, *J. Am. Chem. Soc.*, 2012, **134**, 2930–2933.
11 Z. Zhuang, W. Sheng and Y. Yan, *Adv. Mater.*, 2014, **26**, 3950–3955.
12 G. Mattioli, P. Giannozzi, A. Amore Bonapasta and L. Guidoni, *J. Am. Chem. Soc.*, 2013, **135**, 15353–15363.
13 X. Hao, T. Yan, Z. Wang, S. Liu, Z. Liang, Y. Shen and M. Pritzker, *Thin Solid Films*, 2012, **520**, 2438–2448.
14 Y. Zhang, Q. Xiao, X. Guo, X. Zhang, Y. Xue, L. Jing, X. Zhai, Y. M. Yan and K. Sun, *J. Power Sources*, 2015, **278**, 464–472.
15 Y. Meng, W. Song, H. Huang, Z. Ren, S.-Y. Chen and S. L. Suib, *J. Am. Chem. Soc.*, 2014, **136**, 11452–11464.
16 D. Tang, J. Liu, X. Wu, R. Liu, X. Han, Y. Han, H. Huang and Y. Liu, *ACS Appl. Mater. Interfaces*, 2014, **6**, 7918–7925.
17 X. Long, J. Li, S. Xiao, K. Yan, Z. Wang, H. Chen and S. Yang, *Angew. Chem., Int. Ed.*, 2014, **126**, 7714–7718.
18 X. Li, G. L. Xu, F. Fu, Z. Lin, Q. Wang, L. Huang, J.-T. Li and S. G. Sun, *Electrochim. Acta*, 2013, **96**, 134–140.

